

Sensitivity of polarizations and spin correlations of Z boson to anomalous neutral triple gauge couplings at lepton collider with polarized beams

Amir Subba* and Ritesh K. Singh†

*Department of Physical Sciences,
Indian Institute of Science Education and Research Kolkata,
Mohanpur, 741246, India*

(Dated: December 27, 2023)

We investigate the effects of anomalous neutral triple gauge couplings in ZZ and $Z\gamma$ production processes, followed by the leptonic decay of the Z boson, at a lepton collider with center-of-mass energy $\sqrt{s} = 250$ GeV and polarized beams. We use an effective Lagrangian formalism to parameterize the anomalous couplings in terms of dimension-8 operators $c_{\tilde{B}W}$, c_{BW} , c_{WW} , and c_{BB} , and study the sensitivity of observables such as cross section, polarization, and spin correlation as functions of these couplings. We perform a Bayesian statistical analysis using Markov Chain Monte Carlo methods to determine simultaneous limits on the anomalous couplings, taking into account various luminosities $\mathcal{L} \in \{0.1 \text{ ab}^{-1}, 0.3 \text{ ab}^{-1}, 1 \text{ ab}^{-1}, 3 \text{ ab}^{-1}, 10 \text{ ab}^{-1}\}$ and systematic uncertainties. We find that polarization and spin correlation observables significantly enhance the sensitivity to anomalous couplings, providing stringent constraints on these couplings.

I. INTRODUCTION

The Standard Model (SM) of particle physics is a marvel of scientific achievement. It has undergone rigorous experimental scrutiny to emerge as the most extensively tested theory of fundamental particles and their interactions. The discovery of scalar $J^P = 0^+$ boson by ATLAS [1] and CMS [2] collaborations at LHC consistent with the Standard Model Higgs boson completes the particle spectrum of SM. However, some unresolved issues exist within the SM framework, including fine-tuning the Higgs boson mass, which is susceptible to higher-order quantum corrections that could shift the mass away from the experimental value of 125 GeV. Another unresolved issue is the strong-CP problem, which refers to the unexplained value of the theta parameter (θ) in the quantum chromodynamics (QCD) sector of the SM. Furthermore, dark matter [3], which constitutes approximately 85% of the matter in the Universe, remains a mystery, and its structure still needs to be fully understood. Explaining the non-zero mass of neutrinos and the transformation between the three generations of neutrinos requires physics beyond SM. Recent measurements of the W boson mass [4] and the magnetic moment of the muon [5] have shown significant deviations from the SM. Several models have been proposed to address these shortcomings, such as supersymmetry, technicolor, universal extra dimensions, and string theory, which incorporate extra dimensions, new symmetries, and new particles. However, no experimental evidence has yet confirmed any of these models.

In the absence of any signature in favor of specific models, one adopts a model-independent framework to parameterize the effects beyond the Standard Model, known as the effective field theory (EFT) [6–8] approach. This approach extends the SM Lagrangian by adding higher-order gauge invariant terms constructed from SM states. In general, if a field theory contains a set of fields A and B , where A is light, and B are heavy states, then the action $\tilde{S}[A]$ of the effective field theory may be obtained from the action $\mathcal{S}[A, B]$ of the full field theory by a functional integral over B , $e^{i\tilde{S}[A]} = \int [dB] e^{i\mathcal{S}[A, B]}$. One of the issues with this indirect formalism is the possibility of matching low energy theory to multiple UV complete theory. Such ambiguities are removed only with the discovery of new particles. Usually, the EFT approach remains valid upto some characteristic energy scale, Λ , such that $\Lambda > M_{EW}$, M_{EW} is the electroweak scale. Each higher dimensional terms ($d > 4$) are weighted by Λ^{d-4} power, such that the effective Lagrangian is,

$$\mathcal{L}_{\text{eff}} = \mathcal{L}_{\text{SM}} + \frac{1}{\Lambda^2} \sum_i c_i^{(6)} \mathcal{O}_i^{(6)} + \frac{1}{\Lambda^4} \sum_i c_i^{(8)} \mathcal{O}_i^{(8)} + \dots, \quad (1)$$

where the sum over i runs over a basis $\{\mathcal{O}_i^{(d)}\}$ in the $d \in \{6, 8, 10, \dots\}$ -dimension gauge-invariant operator space and c 's are Wilson coefficients related to those operators. Since the scale of new physics is in several TeV, the higher order terms are highly suppressed; thus, we can safely truncate the expansion in Eq. (1) to some lowest order for collider energy of few TeVs. The presence of these operators affects various structures like couplings of bosons and fermions, and the vacuum expectation value of the Higgs field. The deviation in these structures can be experimentally probed through measurements of various observables.

The SM non-abelian $SU(2) \times U(1)$ gauge structure

* as19rs008@iiserkol.ac.in

† ritesh.singh@iiserkol.ac.in

induces triple and quartic gauge boson couplings. Studies of triple and quartic couplings between the gauge bosons test the SM description of gauge sector interactions and provide sensitivity to physics beyond the SM by examining production rates and kinematics. In the case of triple gauge couplings, the structure SM allows is W^-W^+V , $V \in \{\gamma, Z\}$, and no neutral triple gauge couplings (NTGC) at tree level. At the lowest order, such charged triple gauge boson couplings are affected by dimension-6 operators, while NTGC is generated by dimension-8 operators [9] at the tree level. Besides operator formalism, anomalous NTGC (aNTGC) can also be parameterized as effective vertex. Assuming only Lorentz and $U(1)_{\text{em}}$ gauge invariance, the most general $V_1V_2V_3$ vertex function, where $V_{2,3}$ are on-shell neutral gauge bosons, while $V_1 \in \{Z^*, \gamma^*\}$ is off-shell, can be

written as [10, 11],

$$\begin{aligned} ie\Gamma_{VZZ}^{\alpha\beta\gamma}(q_1, q_2, q_3) &= \frac{-e(q_1^2 - m_V^2)}{m_Z^2} [f_4^V (q_1^\alpha g^{\mu\beta} + q_1^\beta g^{\mu\alpha}) \\ &\quad - f_5^V \epsilon^{\mu\alpha\beta\rho} (q_2 - q_3)_\rho], \\ ie\Gamma_{VZ\gamma}^{\alpha\beta\mu}(q_1, q_2, q_3) &= \frac{-e(q_1^2 - m_V^2)}{m_Z^2} [h_1^V (q_3^\nu g^{\alpha\beta} - q_3^\alpha g^{\mu\beta}) \\ &\quad + \frac{h_2^V}{m_Z^2} q_1^\alpha (q_1 q_3 g^{\mu\beta} - q_3^\mu q_1^\beta) \\ &\quad - h_3^V \epsilon^{\mu\alpha\beta\rho} q_{3\rho} - \frac{h_4^V}{m_Z^2} q_1^\nu \epsilon^{\mu\beta\rho\sigma} q_{1\rho} q_{3\sigma}], \end{aligned} \quad (2)$$

where $V \in \{Z, \gamma\}$. The effective Lagrangian generating the above two vertices is,

$$\begin{aligned} \mathcal{L} &= \frac{e}{m_Z^2} \left[-[f_4^\gamma (\partial_\mu F^{\mu\beta}) + f_4^Z (\partial_\mu Z^{\mu\beta})] Z_\alpha (\partial^\alpha Z_\beta) + [f_5^\gamma (\partial^\sigma F_{\sigma\mu}) + f_5^Z (\partial^\sigma Z_{\sigma\mu})] \tilde{Z}^{\mu\beta} Z_\beta - [h_1^\gamma (\partial^\sigma F_{\sigma\mu}) + h_1^Z (\partial^\sigma Z_{\sigma\mu})] Z_\beta F^{\mu\beta} \right. \\ &\quad - [h_3^\gamma (\partial_\sigma F^{\sigma\rho}) + h_3^Z (\partial_\sigma Z^{\sigma\rho})] Z^\alpha \tilde{F}_{\rho\alpha} - \left. \left\{ \frac{h_2^\gamma}{m_Z^2} [\partial_\alpha \partial_\beta \partial^\rho F_{\rho\mu}] + \frac{h_2^Z}{m_Z^2} [\partial_\alpha \partial_\beta (\square + m_Z^2) Z_\mu] \right\} Z^\alpha F^{\mu\beta} \right. \\ &\quad \left. + \left\{ \frac{h_4^\gamma}{2m_Z^2} [\square \partial^\sigma F^{\rho\alpha}] + \frac{h_4^Z}{2m_Z^2} [(\square + m_Z^2) \partial^\sigma Z^{\rho\alpha}] \right\} Z_\sigma \tilde{F}_{\rho\alpha} \right], \end{aligned} \quad (3)$$

where $\tilde{V}_{\mu\nu} = \frac{1}{2} \epsilon_{\mu\nu\rho\sigma} V^{\rho\sigma}$ ($\epsilon^{0123} = +1$) and the field tensor is defined as $Z_{\mu\nu} = (\partial_\mu Z_\nu - \partial_\nu Z_\mu)$ and $F_{\mu\nu} = (\partial_\mu A_\nu - \partial_\nu A_\mu)$. The couplings f_4^V, h_1^V, h_2^V correspond to the CP -odd tensorial structures, while f_5^V, h_3^V, h_4^V corresponds to the CP -even ones. The above vertex formalism is used to parameterize aNTGC by many experiments like LEP [12–14], LHC [15–17], and Tevatron [18, 19]. Following Ref. [9], there are one CP -even and three CP -odd dimension-8 operators that generates anomalous $ZVV, V \in \{Z^*, \gamma^*\}$ couplings, they are,

$$\begin{aligned} \mathcal{O}_{\tilde{B}W} &= i\Phi^\dagger \tilde{B}_{\mu\nu} W^{\mu\rho} \{D_\rho, D^\nu\} \Phi, \\ \mathcal{O}_{BW} &= i\Phi^\dagger B_{\mu\nu} W^{\mu\rho} \{D_\rho, D^\nu\} \Phi, \\ \mathcal{O}_{WW} &= i\Phi^\dagger W_{\mu\nu} W^{\mu\rho} \{D_\rho, D^\nu\} \Phi, \\ \mathcal{O}_{BB} &= i\Phi^\dagger B_{\mu\nu} B^{\mu\rho} \{D_\rho, D^\nu\} \Phi. \end{aligned} \quad (4)$$

Here, Φ is the Higgs doublet, covariant derivative, $D_\mu = \partial_\mu + \frac{i}{2} g' B_\mu + ig \frac{\sigma_a}{2} W_\mu^a$, field tensor is defined as, $B_{\mu\nu} = \partial_\mu B_\nu - \partial_\nu B_\mu$ and $W_{\mu\nu} = (\partial_\mu W_\nu^a - \partial_\nu W_\mu^a + g\epsilon_{abc} W_\mu^b W_\nu^c)$. In Eq. (4), the first operator is CP -even, and the rest are all CP -odd operators. These operators are suppressed by a fourth power of the new physics scale Λ , which is assumed to be in several TeV, implying the deviation due to these operators are tiny. The matrix element in the presence of these operators is

$$|M|^2 = |M_{SM}|^2 + 2\mathcal{R}(M_{SM} M_8^*) + |M_8|^2. \quad (5)$$

Most of the contribution to the anomalous factor comes from the interference of SM with dimension-8 operators, which is the second term of the above equation. In this article, we work to the order of $1/\Lambda^8$ contribution from dimension-8 operators while keeping all other higher-order operator parameters to zero. Despite not inducing aNTGC at the tree level, the dimension-6 operators can nevertheless have an impact at the one-loop level. The one-loop contributions from the dimension-6 operators would be of the order of $(\alpha/4\pi)(s/\Lambda^2)$, while the contribution from the dimension-eight operators at the tree level would be of the order of (sv^2/Λ^4) . Due to this, for $\Lambda \leq 2v\sqrt{\pi/\alpha} \approx 10$ TeV, the contribution of the dimension-eight operators outweighs the one-loop contribution of the dimension-6 operators [9] and hence ignored in this work.

The anomalous parameters f 's and h 's of the Eq. (3) can be expressed using the Wilson coefficient of dimension-8 operator. We define the related Wilson coefficient of effective operators in Eq. (4) as,

$$c_i \in \{c_{\tilde{B}W}, c_{BW}, c_{WW}, c_{BB}\}. \quad (6)$$

For a process with two on-shell Z bosons, the CP -even couplings are related to Wilson coefficient c_i of effective

operators as [9],

$$\begin{aligned} f_5^Z &= 0, \\ f_5^\gamma &= \frac{v^2 m_Z^2}{4c_W s_W} \frac{c_{\tilde{B}W}}{\Lambda^4}, \end{aligned} \quad (7)$$

where c_W and s_W are cosine and sine of weak mixing angle, respectively. The CP -odd couplings are translated via,

$$\begin{aligned} f_4^Z &= \frac{m_Z^2 v^2}{2c_W s_W} \left[c_W^2 \frac{c_{BB}}{\Lambda^4} + 2c_W s_W \frac{c_{BW}}{\Lambda^4} + 4s_W^2 \frac{c_{WW}}{\Lambda^4} \right], \\ f_4^\gamma &= -m_Z^2 v^2 \left[-c_W s_W \frac{c_{BB}}{\Lambda^4} + \frac{c_{BW}}{\Lambda^4} (c_W^2 - s_W^2) \right. \\ &\quad \left. + 4c_W s_W \frac{c_{WW}}{\Lambda^4} \right]. \end{aligned} \quad (8)$$

For one on-shell Z boson and one on-shell γ , the CP -even couplings are

$$\begin{aligned} h_3^Z &= \frac{v^2 m_Z^2}{4c_W s_W} \frac{c_{\tilde{B}W}}{\Lambda^4} \\ h_4^Z &= h_3^\gamma = h_4^\gamma = 0, \end{aligned} \quad (9)$$

while the CP -odd couplings are related as,

$$\begin{aligned} h_1^Z &= \frac{m_Z^2 v^2}{4c_W s_W} \left[-c_W s_W \frac{c_{BB}}{\Lambda^4} + \frac{c_{BW}}{\Lambda^4} (c_W^2 - s_W^2) \right. \\ &\quad \left. + 4c_W s_W \frac{c_{WW}}{\Lambda^4} \right], \\ h_1^\gamma &= \frac{-m_Z^2 v^2}{4c_W s_W} \left[s_W^2 \frac{c_{BB}}{\Lambda^4} - 2s_W c_W \frac{c_{BW}}{\Lambda^4} + 4c_W^2 \frac{c_{WW}}{\Lambda^4} \right], \\ h_2^Z &= h_2^\gamma = 0. \end{aligned} \quad (10)$$

It is useful to notice that not all anomalous couplings, f_i^V, h_i^V , are independent; given two processes, there are specific relations between those couplings that hold. This is evident from Eq. (7)-(10).

$$\begin{aligned} f_5^\gamma &= h_3^Z, \\ f_4^\gamma &= 4c_W s_W h_1^Z. \end{aligned} \quad (11)$$

Thus the four Wilson's coefficient of dimension-8 operators can be related to and translated to four independent anomalous couplings, $\{f_5^\gamma, f_4^\gamma, f_4^Z, h_1^\gamma\}$. We discuss the behaviour of these anomalous couplings in Appendix A. The effect of higher order operators of Eq. (4) is studied by creating a Universal FeynRules Output (UFO) [20] model files by implementing those operators in FeynRules [21]. This model file was used for event generation in MadGraph5_aMC@NLO [22, 23] in the presence of aNTGC. The input parameters of the model are:

$$\begin{aligned} m_t &= 172.0 \text{ GeV}, & m_Z &= 91.187 \text{ GeV}, \\ m_H &= 125.0 \text{ GeV}, & \alpha_{EW} &= \frac{1}{127.9}, \\ G_F &= 1.166 \times 10^{-5} \text{ GeV}^{-2}, & \alpha_s &= 0.118. \end{aligned} \quad (12)$$

This article aims to provide the sensitivity of various observables like cross section, polarization, and spin correlation asymmetries to the anomalous couplings c_i and to obtain the bounds on these couplings. Similar studies [24–26] used these spin-related observables to constrain anomalous couplings in the neutral and charged sector. The studies had shown significant sensitivity of such observables to new couplings in the case of charged triple gauge couplings [24].

Future lepton colliders like ILC [27, 28], CLIC [29], and FCC-ee [30] will collide the polarized beams, increasing the signal statistics by improving the signal vs. background ratio. Due to the differing weak quantum numbers of left- and right-chiral fermions, they couple differently with the weak gauge bosons. In general, the polarized cross section is written as:

$$\sigma(\eta_3, \chi_3) = \frac{(1 + \eta_3)(1 + \chi_3)}{4} \sigma_{LR} + \frac{(1 - \eta_3)(1 - \chi_3)}{4} \sigma_{RL}, \quad (13)$$

where η_3 and χ_3 are the longitudinal degree of polarization of electron and positron beam, respectively, and $\sigma_{LR}(\sigma_{RL})$ are cross section for 100% left polarized (right polarized) electron beam and 100% right polarized (left polarized) positron beam. The effect of initial beam polarization for ZZ production at e^-e^+ collisions are also studied at one loop electroweak corrections together with soft and hard QED radiation [31].

Here, we probe ZZ , and $Z\gamma$ production followed by the leptonic decay of Z bosons in a e^-e^+ collider, the process is defined as:

$$e^- + e^+ \rightarrow Z + Z \rightarrow e^- e^+ \mu^- \mu^+, \quad (14)$$

and

$$e^- + e^+ \rightarrow Z + \gamma \rightarrow l^- l^+ \gamma. \quad (15)$$

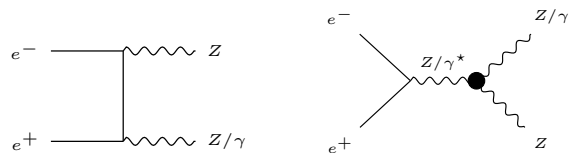


FIG. 1. Representative Feynman diagrams for the production of two neutral boson in SM (left panel) and presence of new physics would also induce a triple neutral gauge boson coupling shown in black blob in right panel.

The degree of polarization used are $\pm 80\%$ for electron and $\pm 30\%$ for positron. The values are taken to be commensurate with the initial plan of ILC [27]. Though we limit the current study to longitudinal polarized beams, the literature on transverse polarized beams can

be found in Refs. [32–38]. The $ZZ \rightarrow 4l$ process in SM happens through electron exchange t and u channel, shown in left panel of Fig. 1. Additional, γ/Z s -channel diagrams are included in presence of dimension-8 operators defined in Eq. (4), which generates neutral triple gauge couplings (ZZZ^* , $ZZ\gamma^*$), shown in right panel of Fig. 1. The $ZZ \rightarrow 4l$ process is minimally diluted by background, and the events are kinematically reconstructable but suffer low statistics due to small branching fractions. As for $l^-l^+\gamma$, $l^- \in \{e^-, \mu^-\}$, it can happen with the photon as a result of initial state radiation (ISR) and leptons from the decay of s -channel mediated by Z boson and γ , apart from the signal in consideration which is the production of $Z\gamma$ through s -channel mediated by Z and γ . Some other diagrams contributing to these kinds of final state topology at the leading order are the production of pair of lepton through s -channel and subsequent final state radiation (FSR). Also, it can proceed with the pair production of photons, with one of the photons being highly off-shell. However, we can suppress non-resonance contributions by imposing the Z -pole event selection condition on e^-e^+ invariant mass. We do not include the detector effects in our analysis for simplicity and because such effects are relatively smaller for e^\pm, μ^\pm , and photon.

The production of ZZ diboson leading to $4l$ final state has been studied at Large Electron-Positron (LEP) Collider [12–14, 39–41] where limits on aNTGC are provided in terms of parameters given in Eq. (3). Several studies were also presented CDF [19, 42], D0 [18, 43], ATLAS [44, 45] and CMS [46] collaborations. On the phenomenological side, aNTGC is extensively studied in Refs. [9, 25, 26, 47–59]. The list of tightest one parameter limits at 95% confidence level (CL) obtained at LHC by ATLAS collaboration in $ZZ \rightarrow 4l$ and $Z\gamma \rightarrow \nu\bar{\nu}\gamma$ final events is given in Table I.

TABLE I. Observed one dimensional 95% confidence level (CL) limits on $c_{\tilde{B}W}$, c_{BW} , c_{WW} and c_{BB} EFT parameters from ATLAS collaboration in LHC.

Parameters (c_i)	Limits (TeV^{-2})	
	$ZZ \rightarrow 4l$ [44]	$Z\gamma \rightarrow \nu\bar{\nu}\gamma$ [45]
$c_{\tilde{B}W}/\Lambda^4$	[-5.9, +5.9]	[-1.10, +1.10]
c_{BW}/Λ^4	[-3.0, +3.0]	[-2.30, +2.30]
c_{WW}/Λ^4	[-3.3, +3.3]	[-0.64, +0.64]
c_{BB}/Λ^4	[-2.7, +2.8]	[-0.24, +0.24]

The aim of the present work is to study the potential of future lepton collider i.e, ILC to probe the various higher dimensional operators inducing aNTGC discussed above at $\sqrt{s} = 250$ GeV. We exploit the spin related observables like polarizations and spin correlations to constrain the anomalous parameters. The construction of those observables in $\nu\bar{\nu}\gamma$ events becomes non-trivial due to the combinatorial issue in reconstructing two missing neutrinos. In the case of $ZZ \rightarrow 4l$, we recon-

struct the polarizations of the Z bosons as well as the spin correlations of two Z bosons. While for the $Z\gamma$ process, we focus only on the polarization of the Z boson as the reconstruction of polarizations of a photon is not possible in collider experiments.

The plan of the paper is as follows: in Sec. II, we discuss the spin of a particle and the observables obtained using the spin. We focus on the asymmetries related to the polarization and spin-spin correlation of Z bosons. In Sec. III, we discuss the limits of anomalous couplings. We conclude in Sec. IV.

II. OBSERVABLES: POLARIZATIONS AND SPIN-SPIN CORRELATIONS

The spin of a particle dictates the couplings with other fermions and bosons. These couplings are affected by the presence of higher-order operators; thus, understanding these couplings will serve as a window to probe deviations from the prediction of SM. The change in couplings may induce deviation in the values of various observables like cross section, momenta, and angular distribution of final state particles. Some of the asymmetries constructed out of the angular distribution of final particles carry information on the spin of the mother particle in the form of polarization parameters. The polarization parameters are related to the dynamics of particle production; thus, these coefficients or spin-related observables can serve as a valuable tool for constraining the parameters of new physics. Generally, a particle with spin- s provides $4s(s+1)$ polarization parameters, which are the independent parameters of the particle spin density matrix. For a spin-1 particle like Z boson, the spin density matrix can be parameterized in Cartesian form as,

$$P(\lambda, \lambda') = \frac{1}{3} \left[I + \frac{3}{2} \vec{P} \cdot \vec{S} + \sqrt{\frac{3}{2}} T_{ij} \{S_i, S_j\} \right], \quad (16)$$

where \vec{P} and T_{ij} are the vector and tensor polarization parameters of Z boson respectively and \vec{S} is the spin-1 operator. To estimate them, one can calculate the parameters from the production density matrix, which is proportional to the product of the production amplitudes for different helicities of the Z boson, $\rho(\lambda, \lambda') \propto M(\lambda)M^*(\lambda')$, where $\lambda \in \{-, 0, +\}$. Alternatively, one can constraint them at the decay level using the angular distribution of the decay products as in collider experiments. In this article, we focus on constructing polarization of Z boson using the later methods. The angular distribution of fermions decayed from a spin-1 boson is

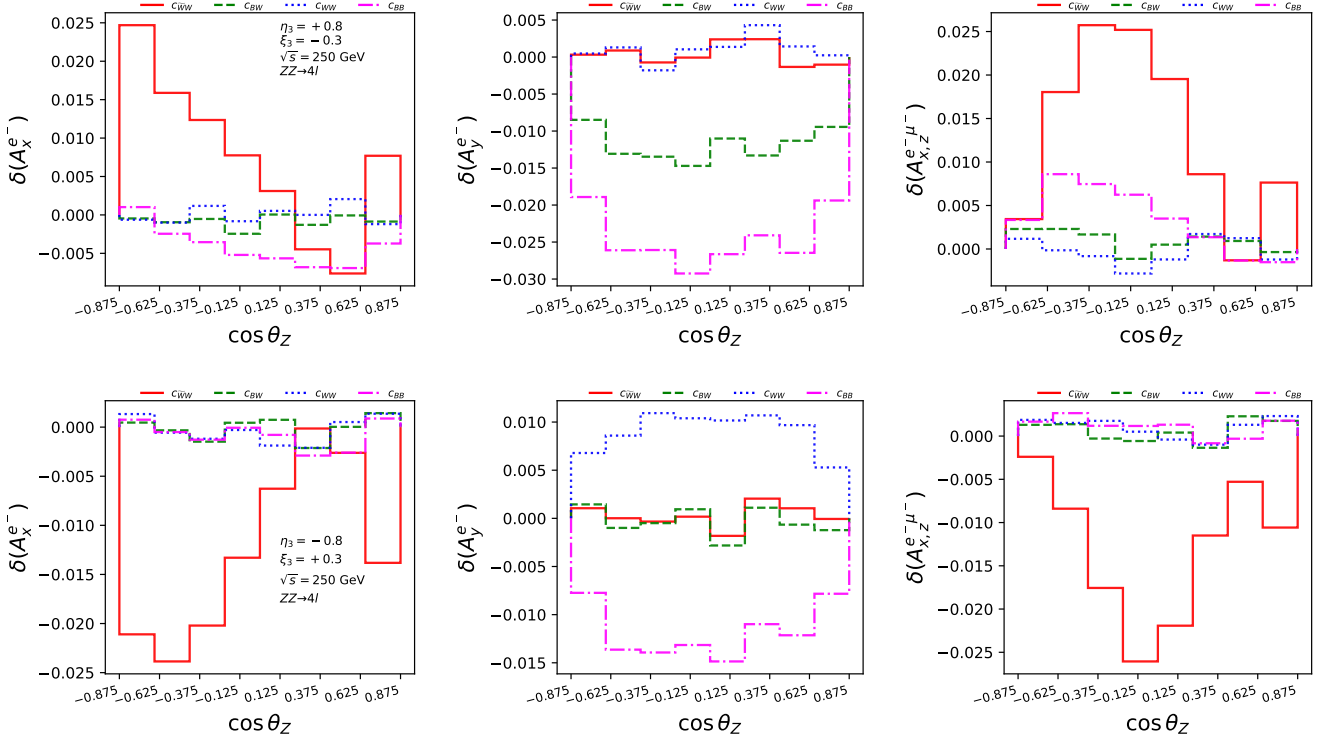


FIG. 2. Relative change in asymmetries related to the CP-even (P_x) and CP-odd (P_y) polarization and correlation ($A_{x,z}$) where both the functions are CP-even. The distributions are shown for two set of beam polarization, $\eta_3, \xi_3 = +0.8, -0.3$ (in the top row) and the flipped polarization (in the bottom row) for four different anomalous couplings. The analysis is done at $\sqrt{s} = 250$ GeV, and at the rest frame of the mother particle.

written as [60],

$$\begin{aligned}
\frac{1}{\sigma} \frac{d\sigma}{d\Omega} = & \frac{3}{8\pi} \left[\left(\frac{2}{3} - (1-3\delta) \frac{T_{zz}}{\sqrt{6}} \right) + \alpha P_z \cos \theta \right. \\
& + \sqrt{\frac{3}{2}} (1-3\delta) T_{zz} \cos^2 \theta + \left(\alpha P_x + 2\sqrt{\frac{2}{3}} (1-3\delta) T_{xz} \cos \theta \right) \\
& \times \sin \theta \cos \theta + \left(\alpha P_y + 2\sqrt{\frac{2}{3}} (1-3\delta) T_{yz} \cos \theta \right) \sin \theta \sin \phi \\
& + (1-3\delta) \sin^2 \theta \left\{ \left(\frac{T_{xx} - T_{yy}}{\sqrt{6}} \right) \cos(2\phi) \right. \\
& \left. + \sqrt{\frac{2}{3}} T_{xy} \sin(2\phi) \right\} \left. \right]. \tag{17}
\end{aligned}$$

Here, θ, ϕ are the polar and azimuthal angle of the final state fermion in the rest frame of the Z boson with its would-be momentum along the z -direction and $x-z$ plane being the lab frame production plane. The parameters α and δ depend on the chiral couplings and ratio of the mass of final state fermions to the mass of resonance, such that at the limit of massless fermions, $\alpha \rightarrow \frac{R_f^2 - L_f^2}{R_f^2 + L_f^2}$ and $\delta \rightarrow 0$ [60]. At the decay level, one can calculate various asymmetries related to polarization and spin cor-

relation parameters by taking the partial integration of Eq. (17) w.r.t θ and ϕ . For example, we can get P_x from the left-right asymmetry as [60],

$$\begin{aligned}
A_x = & \frac{1}{\sigma} \left[\int_{\theta=0}^{\pi} \int_{\phi=-\frac{\pi}{2}}^{\frac{\pi}{2}} \frac{d\sigma}{d\Omega} d\Omega - \int_{\theta=0}^{\pi} \int_{\phi=\frac{\pi}{2}}^{3\frac{\pi}{2}} \frac{d\sigma}{d\Omega} d\Omega \right] \tag{18} \\
= & \frac{3\alpha P_x}{4} = \frac{\sigma(f_x > 0) - \sigma(f_x < 0)}{\sigma(f_x > 0) + \sigma(f_x < 0)},
\end{aligned}$$

where $f_x = \sin \theta \cos \phi$. Likewise, the other angular functions used to construct the asymmetries are $f_y = \sin \theta \sin \phi$, $f_z = \cos \theta$, $f_{xy} = f_x f_y$, $f_{xz} = f_x f_z$, $f_{yz} = f_y f_z$, $f_{x^2-y^2} = f_x^2 - f_y^2$, and $f_{zz} = \sqrt{1-f_z^2} [3-4(1-f_z^2)]$. The asymmetries related to other polarization parameters are obtained similarly using the above function.

When two particles are co-produced, their spin is correlated owing to the conservation of angular momentum. In general, for two particles A and B with spin s_A and s_B respectively, there are $16s_A s_B (s_A + 1)(s_B + 1)$ spin correlation parameters. The total rate for the production of two spin-1 particles followed by their

decay, i.e, $A \rightarrow aa'$ and $B \rightarrow bb'$ can be written as [61],

$$\frac{1}{\sigma} \frac{d\sigma}{d\Omega_a d\Omega_b} = \frac{9}{16\pi^2} \sum_{\lambda_A, \lambda'_A, \lambda_B, \lambda'_B} P_{AB}(\lambda_A, \lambda'_A, \lambda_B, \lambda'_B) \Gamma_A(\lambda_A, \lambda'_A) \Gamma_B(\lambda_B, \lambda'_B). \quad (19)$$

P_{AB} represents the joint polarization density matrix. Moreover, similarly, by using the respective form for the density matrix, one obtains the joint angular distribution of the decay products of A and B . In the case of two spin-1 particles, there will be 64 spin correlation parameters, which can be obtained using different angular functions as [61],

$$\mathcal{A}_{ij}^{AB} = \frac{\sigma(f_i^a f_j^b > 0) - \sigma(f_i^a f_j^b < 0)}{\sigma(f_i^a f_j^b > 0) + \sigma(f_i^a f_j^b < 0)}. \quad (20)$$

It is worth noting that the asymmetries defined above can be divided into CP-even and CP-odd observables. Three of the polarization asymmetries are CP-odd, and five are CP-even. In the case of spin correlations, there are 34 CP-even and 30 CP-odd asymmetries. In Fig. 2, we show the relative change of asymmetries value in presence of anomalous couplings by keeping one anomalous couplings to non-zero at a time while other are set to zero. The benchmark anomalous point is kept to 100 TeV⁻² for each new physics parameter. In particular, we show the variation for asymmetries (polarization) related to the angular distribution of $f_x^{e^-} (A_x^{e^-})$, $f_y^{e^-} (A_y^{e^-})$ and correlation of function $f_x^{e^-} f_z^{\mu^-} (A_{x,z}^{e^- \mu^-})$. We perform this analysis at center-of-mass energy of 250 GeV, with two set of initial beam polarization $(\eta_3, \xi_3) = (+0.8, -0.3)$ (shown in the top row) and the flipped polarization (in the bottom row). In Fig. 2, we see that the variation in the asymmetries for CP-odd anomalous couplings, $c_i \in \{c_{WW}, c_{BB}, c_{BW}\}$ are minimal while the variation are significant for CP-even asymmetries like A_x , and $A_{x,z}^{e^- \mu^-}$, while it provides significant change in CP-odd asymmetries ($A_y^{e^-}$). Further, in case of CP-even asymmetries the sign of the relative change in asymmetries gets flipped in the case when the beam polarization is flipped. Thus, various asymmetries might act as an analyzer for the CP state of the new physics. The change in the asymmetries due to anomalous couplings are non-symmetric to the $\cos\theta_Z$ related to the Z boson. E.g., in the case of asymmetries related to $A_{x,z}$, the maximal change from the SM value is seen for $-0.5 < \cos\theta_Z < 0.5$ region, and in the case of A_x , the change follows a asymmetric distribution in the range $-1.0 < \cos\theta_Z < +1.0$. This asymmetric change w.r.t $\cos\theta_Z$ allows one to bin the asymmetries in a specific range of $\cos\theta_Z$.

In the next section, we discuss the methodology and the limits obtained on various anomalous couplings. We will also emphasize the role of statistical and

systematic errors in setting the bounds on anomalous couplings.

III. PROBE OF ANOMALOUS COUPLINGS

This section presents a comprehensive methodology for obtaining bounds on anomalous couplings, denoted by c_i , in the context of ZZ and $Z\gamma$ processes. Our approach involves dividing all the observables into eight bins of $\cos\theta_Z$, where θ_Z represents the production angle of the Z boson in the laboratory frame. This allows us to increase the number of observables and better constrain the anomalous couplings. This strategy has the advantage of fine-tuning the distinction between the signal resulting from new physics and the SM forecast. The ability to detect and eliminate differences between the SM predictions and experimental data is made possible by the growth in observables, which in turn allows us to impose stricter limits on anomalous couplings. The event simulations are carried out using the Monte Carlo method implemented in MadGraph5_aMC@NLO [23], which allows us to simulate the production and decay of ZZ and $Z\gamma$ bosons in the presence of anomalous couplings. The resulting simulated events are then analyzed to extract the relevant observables, which are divided into the eight bins mentioned above of $\cos\theta_Z$.

Next, we fit the values of the observables in each bin to derive a semi-analytical expression for all observables as a function of the anomalous couplings. This enables us to establish the relationship between the observables and the anomalous couplings and to derive the most likely values of the couplings that best fit the data. In presence of anomalous couplings, c_i , the cross section is fitted using the following parameterization,

$$\sigma = \sigma_0 + \sigma_i c_i + \sum_{j \neq k} \sigma_{jk} c_j c_k + \sum_{l=1}^4 \sigma_l c_l^2, \quad (21)$$

$$i = c_{\tilde{B}W}, j, k \in \{c_{BW}, c_{WW}, c_{BB}\}, l = i \cup j.$$

The numerator and denominator are fitted independently for asymmetries and then used as

$$\mathcal{A}_i(\{c_i\}) = \frac{\Delta\sigma_{\mathcal{A}_i}(\{c_i\})}{\sigma(\{c_i\})}. \quad (22)$$

The denominator is the cross section which is fitted as in Eq. (21), and the numerator of CP-odd asymmetries is fitted as,

$$\Delta\sigma_{\mathcal{A}_i}(\{c_i\}) = \sum_i \sigma_i c_i + \sum_i \sigma_{1i} c_{\tilde{B}W} c_i, \quad (23)$$

$$i \in \{c_{BW}, c_{WW}, c_{BB}\}.$$

When dealing with events with two sets of beam polarization, merging the different sets at the χ^2 level yields

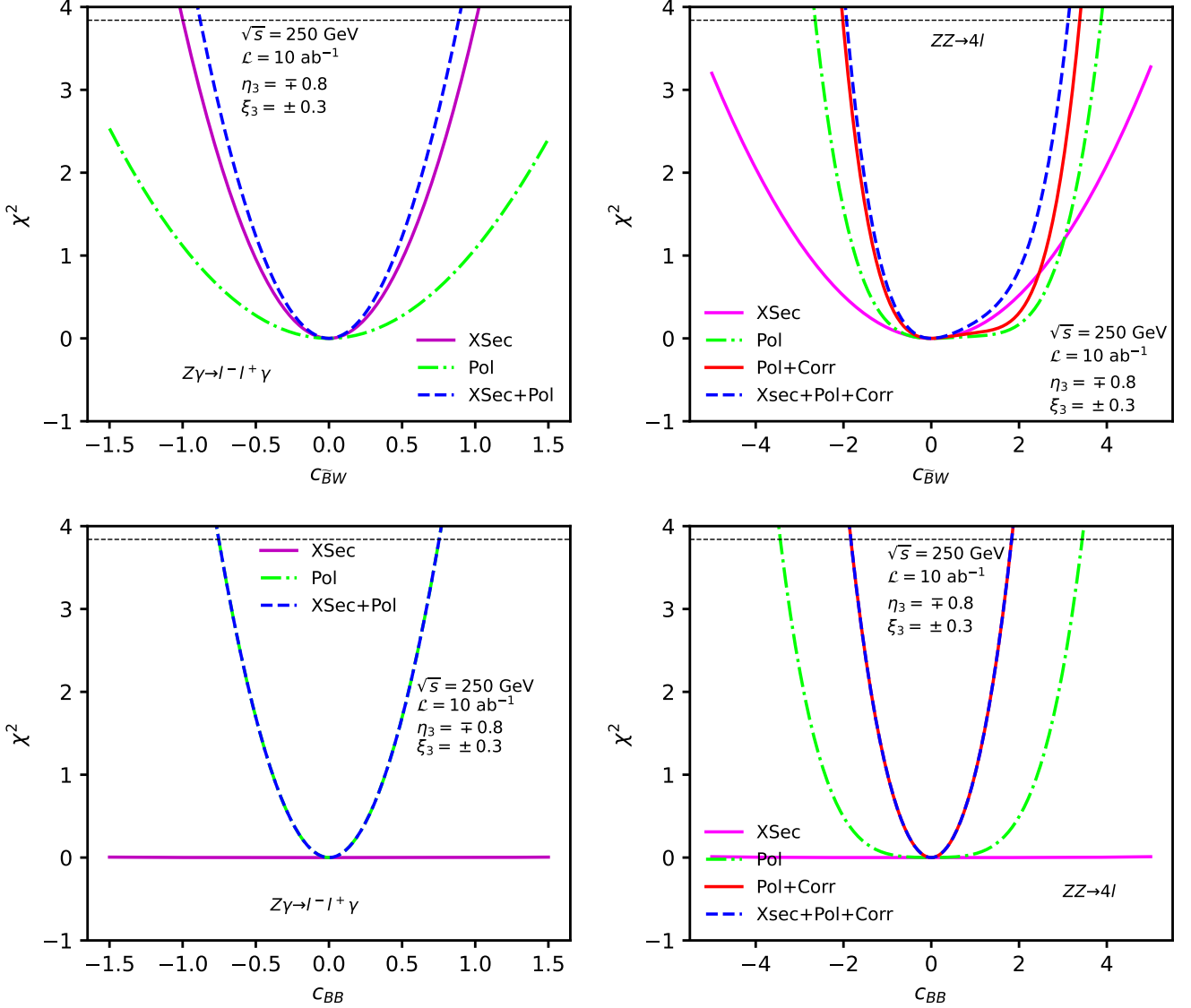


FIG. 3. One dimensional χ^2 for cross-section, polarizations, combinations of polarization and spin-spin correlations and combinations of all observables as a function of one anomalous couplings at a time for a $ZZ \rightarrow 4l$ and $Z\gamma \rightarrow l^-l^+\gamma$ process. The plots are obtained at $\sqrt{s} = 250$ GeV, $\mathcal{L} = 10$ ab $^{-1}$ and zero systematic errors. The horizontal line at $\chi^2 = 3.84$ corresponds to the limits of anomalous couplings at 95% confidence level (CL).

more stringent constraints [62]. The combined χ^2 at different set of beam polarization ($\pm\eta_3, \mp\xi_3$), and using different observable \mathcal{O} for a given value of anomalous couplings c_i is defined as,

$$\chi^2(\mathcal{O}, c_i, \pm\eta_3, \mp\xi_3) = \sum_{l,k} \left[\left(\frac{\mathcal{O}_k^l(c_i, +\eta_3, -\xi_3) - \mathcal{O}_k^l(0, +\eta_3, -\xi_3)}{\delta\mathcal{O}_k^l(0, +\eta_3, -\xi_3)} \right)^2 + \left(\frac{\mathcal{O}_k^l(c_i, -\eta_3, +\xi_3) - \mathcal{O}_k^l(0, -\eta_3, +\xi_3)}{\delta\mathcal{O}_k^l(0, -\eta_3, +\xi_3)} \right)^2 \right], \quad (24)$$

where k, l runs over all bins and observables separately, and $\delta\mathcal{O} = \sqrt{(\delta\mathcal{O}_{\text{stat}})^2 + (\delta\mathcal{O}_{\text{sys}})^2}$ is the estimated error

in \mathcal{O} . For cross section σ , the estimated error is given by,

$$\delta\sigma = \sqrt{\frac{\sigma}{\mathcal{L}} + (\epsilon_\sigma\sigma)^2}, \quad (25)$$

and if the observable is asymmetry, the error is given by,

$$\delta\mathcal{A} = \sqrt{\frac{1 - \mathcal{A}^2}{\mathcal{L}\sigma} + \epsilon_{\mathcal{A}}^2}. \quad (26)$$

Here, $\epsilon_{\mathcal{A}}, \epsilon_\sigma$ are the systematic error in asymmetry and cross section, respectively, and \mathcal{L} is the integrated luminosity. The chi-squared analysis provides complete information on the sensitivity of observables along with the constraint on anomalous couplings. The analysis are

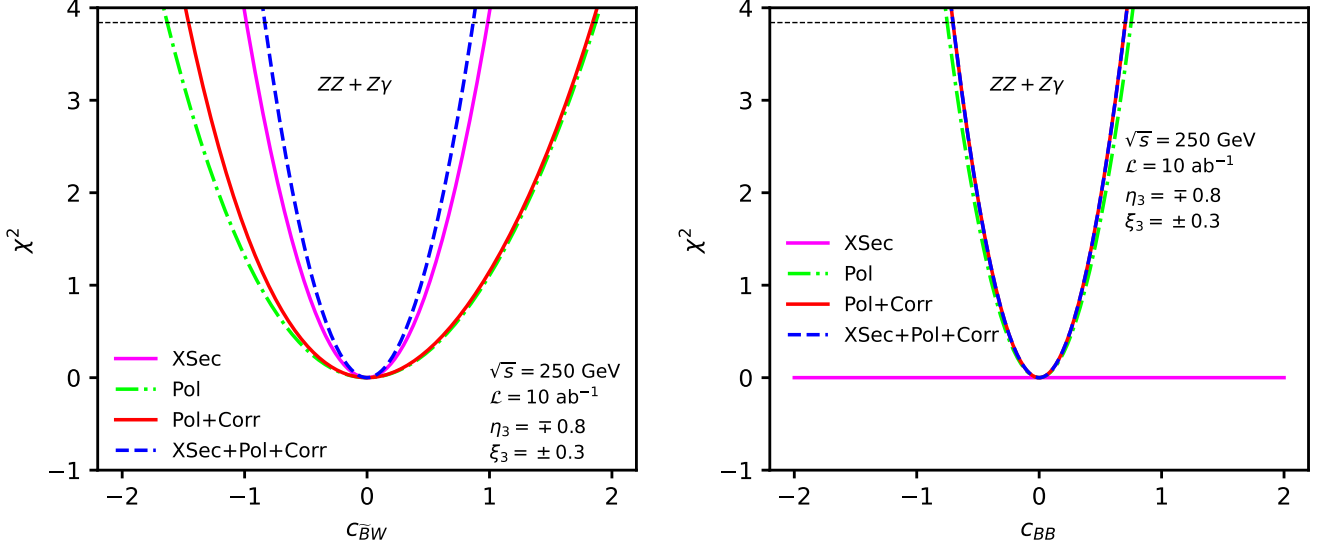


FIG. 4. One dimensional combined χ^2 for different sets of observables as a function of anomalous couplings ($c_i \in \{c_{\bar{B}W}, c_{BW}\}$). The horizontal line at $\chi^2 = 3.84$ denotes limits at 95% CL. The analysis is done with zero systematic error.

performed at $\sqrt{s} = 250$ GeV with different values of integrated luminosity,

$$\mathcal{L} \in \{0.1 \text{ ab}^{-1}, 0.3 \text{ ab}^{-1}, 1 \text{ ab}^{-1}, 3 \text{ ab}^{-1}, 10 \text{ ab}^{-1}\}. \quad (27)$$

The SM cross sections for $ZZ \rightarrow e^-e^+\mu^-\mu^+$ and $Z\gamma \rightarrow l^-l^+\gamma$ process at $\sqrt{s} = 250$ GeV with two set of initial beam polarization of ($\pm 0.8, \mp 0.3$) are,

$$\begin{aligned} \sigma_{ZZ}(+0.8, -0.3) &= 2.15 \text{ fb}, \\ \sigma_{ZZ}(-0.8, +0.3) &= 3.41 \text{ fb}, \\ \sigma_{Z\gamma}(+0.8, -0.3) &= 607.62 \text{ fb}, \\ \sigma_{Z\gamma}(-0.8, +0.3) &= 765.83 \text{ fb}. \end{aligned} \quad (28)$$

Given the cross section as in Eq. (28) and luminosity in Eq. (27), the relative statistical error as obtained from Eq. (25) are,

$$\begin{aligned} \frac{\delta\sigma}{\sigma}(+0.8, -0.3)|_{ZZ} &= \{6.81\%, 3.93\%, 2.15\%, 1.24\%, 0.68\%\}, \\ \frac{\delta\sigma}{\sigma}(-0.8, +0.3)|_{ZZ} &= \{5.40\%, 3.12\%, 1.71\%, 0.98\%, 0.54\%\}, \\ \frac{\delta\sigma}{\sigma}(+0.8, -0.3)|_{Z\gamma} &= \{0.40\%, 0.23\%, 0.12\%, 0.07\%, 0.04\%\}, \\ \frac{\delta\sigma}{\sigma}(-0.8, +0.3)|_{Z\gamma} &= \{0.36\%, 0.20\%, 0.11\%, 0.06\%, 0.03\%\}. \end{aligned} \quad (29)$$

The above statistical error is given for a unbinned events, while for the binned (eight bin) case the statistical error increases depending on the rate. On top of the statistical error given in the above equation, we add systematic error given as,

$$(\epsilon_\sigma, \epsilon_A) = \{(0, 0), (0.5\%, 0.25\%), (2\%, 1\%)\}. \quad (30)$$

In the case of $ZZ \rightarrow 4l$ events, the estimated error is primarily dominated by the statistical component within the regime of systematic error given by Eq. (30) due to the low branching ratio of the full lepton channel. It implies that the sensitivity of various observables would increase with luminosity, while for the case of $Z\gamma$ process the net error saturates for given non-zero value of systematic error.

The figures presented in Fig. 3 depict the χ^2 analysis performed for various sets of observables as a function of one anomalous coupling at a time for two different final topologies: $4l$ and $l^-l^+\gamma$. The analysis is carried with an integrated luminosity of $\mathcal{L} = 10 \text{ ab}^{-1}$, and with systematic errors chosen to be zero. The beams are polarized with a degree of polarization $\eta_3 = \pm 0.8$ and $\xi_3 = \mp 0.3$.

Each panel of Fig. 3 illustrates that the dominant contribution to constraining anomalous couplings arises from the spin-related observables, which are combinations of the polarization and spin-spin correlation parameters. For CP-odd couplings in the bottom row of the Fig. 3, the limits set by these spin-related observables remain unaffected by the presence of a cross section. This is because, in the case of CP-even observables like cross section, the contribution from CP-odd couplings only arises at the $1/\Lambda^8$ term, whose contribution is sub-dominant compared to the linear contribution ($1/\Lambda^4$) from CP-even. In the presence of one anomalous coupling (c_i), the CP-even observables can be parameterized by Eq. (31),

$$\sigma(c_i) = \sigma_0 + \sigma_i c_i + \sigma_{ii} c_i^2, \quad (31)$$

where σ_0 corresponds to the SM value. Therefore, the linear term in the cross section is absent for CP-odd

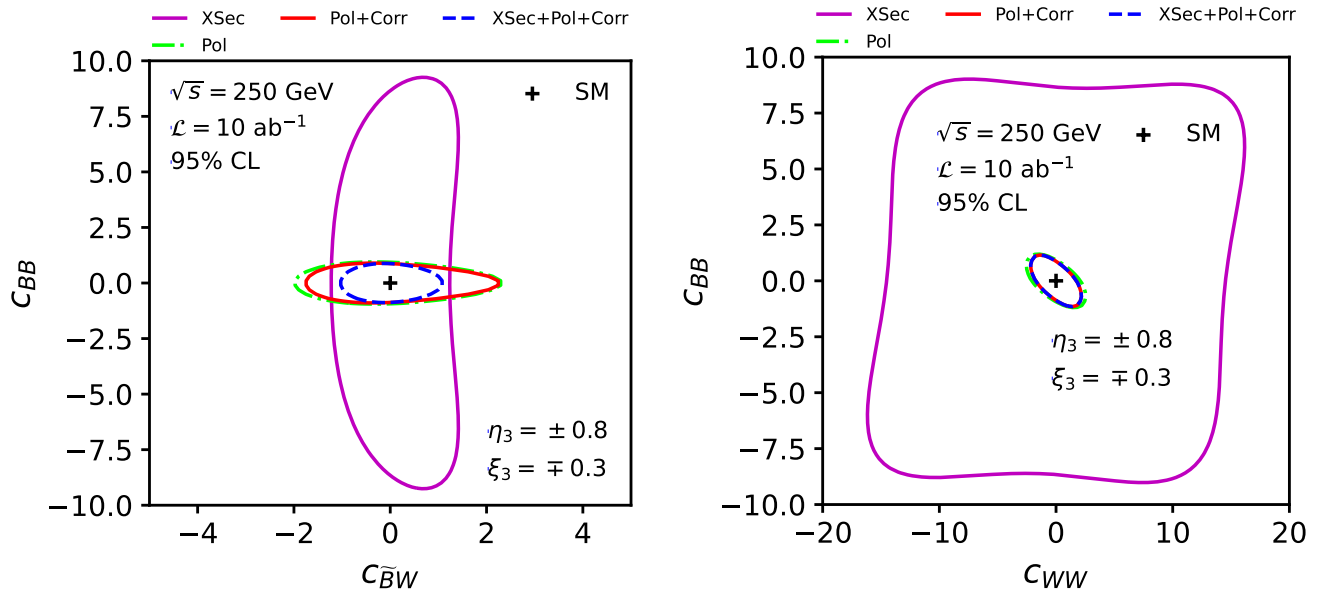


FIG. 5. 2-D 95% CL contours of χ^2 for cross-section, polarizations, spin correlations and their combinations as a function of two anomalous couplings at a time for combined ZZ and $Z\gamma$ process. The analysis is done at center of mass energy $\sqrt{s} = 250$ GeV, integrated luminosity $\mathcal{L} = 10 \text{ ab}^{-1}$ and systematic error are chosen to be zero. The cross in the center represents SM points.

c_i , leading to a negligible contribution. It is also evident from Fig. 3 that the $Z\gamma$ process imposes a tighter constraint than the ZZ process in the case of CP-odd coupling, C_{BB} through combination of different polarization asymmetries. However, for the CP-even case, the cross section provides tighter constraint than the polarization asymmetries in case of $Z\gamma$ process, while the limits for the same anomalous coupling from ZZ process is bit relaxed. Next, we combine the two processes at the level of χ^2 as,

$$\chi_{\text{Tot}}^2(\{c_i\}, \pm\eta_3, \mp\xi_3) = \chi_{ZZ}^2(\{c_i\}, \pm\eta_3, \mp\xi_3) + \chi_{Z\gamma}^2(\{c_i\}, \pm\eta_3, \mp\xi_3), \quad (32)$$

where each χ^2 is obtained following Eq. (24) and on obtaining the above defined χ^2 , we have consider the all other leptonic decay channel for ZZ process. The resultant one and two-dimensional χ^2 distribution for a set of observables as a function of one and two anomalous couplings at a time are shown in Fig. 4 and Fig. 5, respectively. The hierarchy of observables on setting the bounds on anomalous couplings is the same as described above for individual topology. For CP-odd case, the cross section provides the least contribution to the χ^2 , and combinations of polarization and spin correlation asymmetries predominantly set the bounds. For the CP-even case, the cross section contributes the most to χ^2 alone. The one parameter limits at 95% confidence level (CL) obtained from the combined analysis are listed in Table II, where it is evident that the $Z\gamma$ channel dominates the limits on most of the anomalous couplings,

except for c_{BW} . The one parameter limits in the current

TABLE II. One parameter limits on anomalous couplings (c_i) at 95% CL obtained for $ZZ \rightarrow 4l$, $Z\gamma \rightarrow 2l\gamma$ and their combinations. The limits are obtained at center of mass energy $\sqrt{s} = 250$ GeV, integrated luminosity $\mathcal{L} = 10 \text{ ab}^{-1}$ and zero systematic.

Parameters (c_i)	Limits (TeV^{-4})		
	$Z\gamma \rightarrow 2l\gamma$	$ZZ \rightarrow 4l$	$ZZ + Z\gamma$
$c_{\bar{B}W}/\Lambda^4$	[-0.88, +0.88]	[-1.93, +3.11]	[-0.83, +0.86]
c_{BW}/Λ^4	[-2.89, +2.89]	[-2.40, +2.40]	[-1.97, +1.97]
c_{WW}/Λ^4	[-1.75, +1.75]	[-2.17, +2.17]	[-1, 42, +1.42]
c_{BB}/Λ^4	[-0.75, +0.75]	[-1.83, +1.83]	[-0.70, +0.70]

work (ILC @ 10 ab^{-1}) are diluted for $Z\gamma$ process, while the limits are tighter for ZZ process, in contrast to the experimental limit (LHC @ 36.1 fb^{-1}) listed in Table I. Our current study examines the ILC potential to probe dim-8 bosonic operators without directly comparing it to existing colliders. Notably, the LHC boasts a higher collision energy ($\approx 2 \text{ TeV}$) compared to the ILC (250 GeV). This makes the anomalous vertex more sensitive to the higher energy reach of LHC since the vertex created by dim-8 operators comprises the terms reliant on the momentum transfer normalized by the electroweak scale. Besides the energy domination at LHC, the cross-section of $Z\gamma \rightarrow \nu\bar{\nu}\gamma$ is ≈ 25 times larger at ILC than it is for $Z\gamma \rightarrow l^-l^+\gamma$, while for $ZZ \rightarrow 4l$ process the cross section is ≈ 9 times higher in LHC than at ILC. Nevertheless, the significant number of observables used in our analysis try to compensate for the low energy and

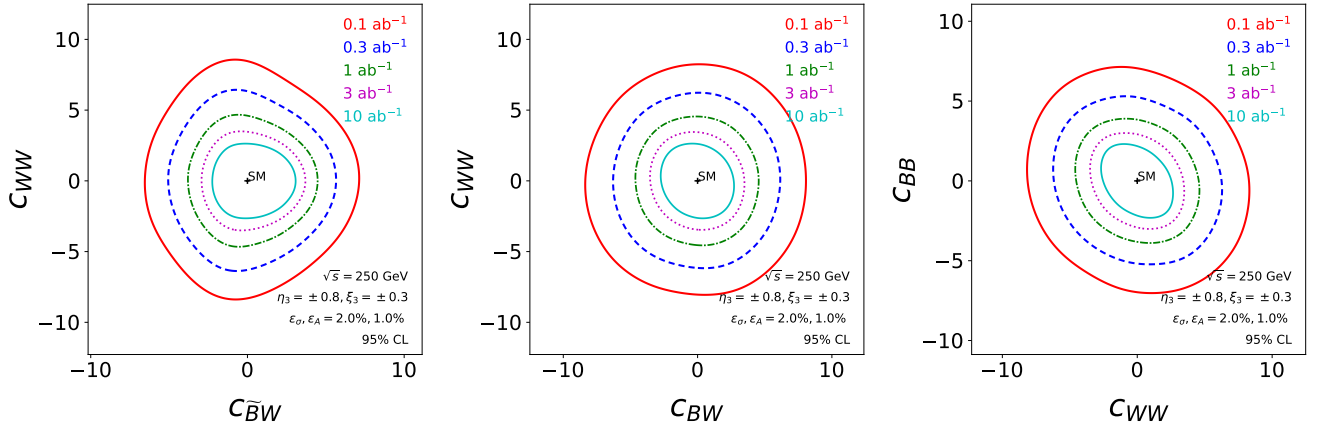


FIG. 6. Two dimensional marginalized projections of the anomalous couplings c_i (TeV^{-4}) at 95% CL obtained using MCMC global fits for a conservative systematic error (2.0%, 1.0%) and different values of integrated luminosities.

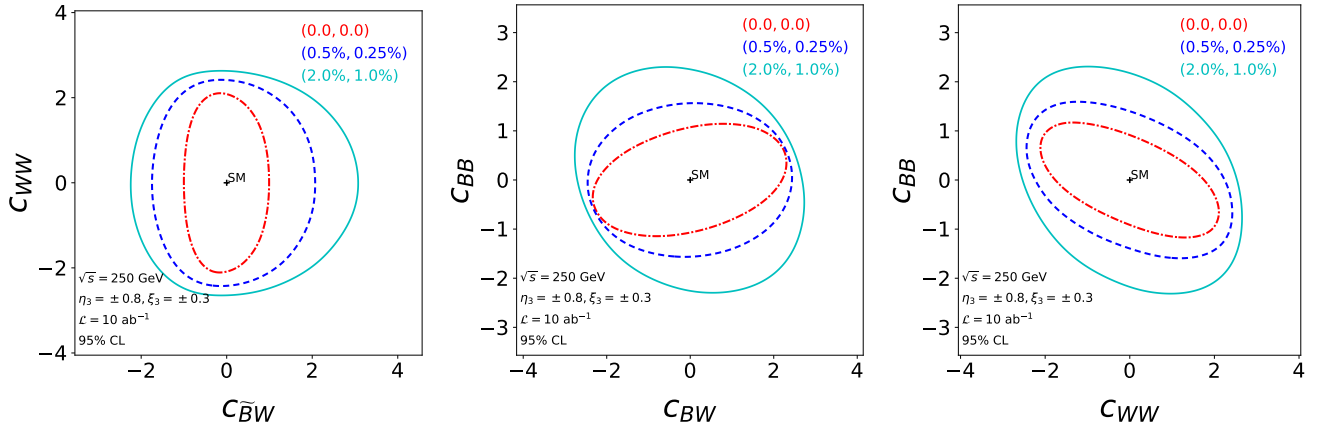


FIG. 7. Two dimensional marginalized projections of the maximally correlated parameters c_i (TeV^{-4}) at 95% CL obtained using MCMC global fits for a set of systematic error and integrated luminosity $\mathcal{L} = 10 \text{ ab}^{-1}$.

cross section, which is visible in Fig. 4 where the limits on anomalous couplings become tighter on using polarizations and spin correlations. A recent study [25] achieved a comparable limit on anomalous couplings at greater energy $\sqrt{s} = 500 \text{ GeV}$, using fewer observables (polarizations of Z bosons). Similar study [59] at LHC at 13 TeV using polarizations of Z boson in final $4l$ events obtained a tighter constraint on anomalous couplings. The higher collision energy compensates for the higher number of observables.

In case of two dimensional contours shown in Fig. 5, the cross section in presence of two anomalous couplings (c_i, c_j) can be parameterized as,

$$\begin{aligned} \sigma_i(c_i, c_j) &= \sigma_0 + \sigma_i c_i + \sigma_{ij} c_i c_j + c_{ii} c_i^2 + c_{jj} c_j^2, \\ c_i &= c_{\bar{B}W}, c_j \in \{c_{BW}, c_{WW}, c_{BB}\}. \end{aligned} \quad (33)$$

As mentioned earlier, when both parameters are CP-odd, the linear term vanishes; in the case of one CP-odd and CP-even parameter, the interference between anomalous parts vanishes. The shape described by Eq.(33) can be

seen in the left panel of Fig. 5, which contains one CP-even and one CP-odd coupling, resulting in tighter constraints on the x-axis than the y-axis. As in the one-parameter case, the spin-related observables have the maximal contribution in simultaneously constraining the two anomalous couplings. The results are provided for the rest of the analysis by combining the two processes as defined in Eq. (32). We conclude our analysis by performing a Markov Chain Monte Carlo (MCMC) computation using two sets of observables for two different polarized beams to derive simultaneous limits on all anomalous couplings (c_i). We aim to determine the likelihood of a given point $\mathbf{c} \in \{c_i, \pm\eta_3, \mp\xi_3\}$ in the parameter space. This is achieved by defining the likelihood function as the product of exponential functions of the χ^2 function evaluated at \mathbf{c} as,

$$\mathcal{L}(\mathbf{c}) = \prod_{i,j} \exp \left[-\frac{\chi^2(\mathbf{c})}{2} \right], \quad (34)$$

TABLE III. List of posterior 95% Bayesian Confidence Interval (BCI) of anomalous couplings for $\sqrt{s} = 250$ GeV with beam polarization $(\eta_3, \xi_3) = (\pm 0.8, \pm 0.3)$ from MCMC global fits at different value of luminosity and systematic error.

\mathcal{L} (fb $^{-1}$)	$(\epsilon_\sigma, \epsilon_A)$	$c_{\tilde{B}W}$ (TeV $^{-4}$)	c_{BW} (TeV $^{-4}$)	c_{WW} (TeV $^{-4}$)	c_{BB} (TeV $^{-4}$)
100	(0.0,0.0)	[-4.81, +5.11]	[-6.83, +6.59]	[-6.64, +6.73]	[-5.31, +5.38]
	(0.5%,0.25%)	[-4.88, +5.21]	[-6.83, +6.60]	[-6.65, +6.74]	[-5.36, +5.42]
	(2.0%,1.0%)	[-5.28, +5.76]	[-6.87, +6.63]	[-6.67, +6.79]	[-5.71, +5.81]
300	(0.0,0.0)	[-3.33, +3.51]	[-5.14, +5.02]	[-5.01, +5.02]	[-3.63, +3.64]
	(0.5%,0.25%)	[-3.51, +3.76]	[-5.14, +5.03]	[-5.04, +5.05]	[-3.73, +3.75]
	(2.0%,1.0%)	[-4.08, +4.61]	[-5.19, +5.06]	[-5.11, +5.13]	[-4.28, +4.33]
1000	(0.0,0.0)	[-2.18, +2.22]	[-3.75, +3.69]	[-3.60, +3.60]	[-2.31, +2.30]
	(0.5%,0.25%)	[-2.49, +2.68]	[-3.76, +3.69]	[-3.67, +3.67]	[-2.49, +2.47]
	(2.0%,1.0%)	[-3.08, +3.69]	[-3.83, +3.75]	[-3.77, +3.77]	[-3.19, +3.21]
3000	(0.0,0.0)	[-1.41, +1.38]	[-2.75, +2.72]	[-2.59, +2.58]	[-1.50, +1.49]
	(0.5%,0.25%)	[-1.88, +2.11]	[-2.79, +2.75]	[-2.74, +2.73]	[-1.76, +1.75]
	(2.0%,1.0%)	[-2.47, +2.91]	[-2.93, +2.88]	[-2.87, +2.86]	[-2.47, +2.47]
10000	(0.0,0.0)	[-0.83, +0.84]	[-1.89, +1.87]	[-1.71, +1.70]	[-0.92, +0.92]
	(0.5%,0.25%)	[-1.48, +1.66]	[-2.01, +1.99]	[-1.99, +1.98]	[-1.28, +1.28]
	(2.0%,1.0%)	[-1.89, +2.48]	[-2.27, +2.48]	[-2.19, +2.18]	[-1.90, +1.90]

where χ^2 is defined in Eq. (24), and the indices i and j respectively run over the list of all bins and observables, including cross sections, polarizations, and spin correlation asymmetries. We perform this analysis for a set of luminosities given in Eq. (27), as well as systematic error given in Eq. (30). The MCMC implementation utilizes the Metropolis-Hastings algorithm. The marginalized limits on the Wilson's coefficient c_i at 95% CL is listed in Table III for different values of integrated luminosity and systematic errors.

Fig. 6 illustrates the two-dimensional marginalized projections at a 95% CL for the anomalous couplings (c_i) obtained from the MCMC global fits for a systematic error of (2%,1%) and different luminosity values listed in Eq. (27). On increasing the luminosity from 0.1 fb $^{-1}$ to 10 fb $^{-1}$, the limits on each anomalous couplings gets better by an approximate factor of 3. For a case of zero systematic, the limits gets better by a factor of ≈ 6 on increasing the luminosity by a factor of 100 while in case of a moderate systematic error (0.5%,0.25%), the limits gets tightened by nearly a factor of 3.4 with the same range of luminosity. Thus, the results points that the reduction of systematic errors becomes very important for the probe of the aNTGC.

To comprehensively comprehend the impact of systematic error on constraining anomalous couplings, we analyze two-dimensional marginalized projections of anomalous couplings with a luminosity of $\mathcal{L} = 10$ ab $^{-1}$ (see Fig. 7). In middle panel which

depicts a pair plot of (c_{BW}, c_{BB}) , it is observed that the systematic errors have a minor impact on the marginalized limits of c_{BW} coupling. It is due to a large statistical error associated with the $ZZ \rightarrow 4l$ process, and this process predominantly sets the bounds on c_{BW} through its large number of spin-related observables. The improvement on the limits of c_{WW} is ≈ 1.28 , while for $c_{\tilde{B}W}$, and c_{BB} the limits improved by a factor of 2.3 and 2.1, respectively.

The marginalized limits suggest that the higher luminosity and lower systematic errors becomes of paramount importance to probe the non-standard triple gauge boson couplings in future lepton collider like ILC. The current study involved the leptonic decay of Z boson, which has a low branching ratio. Analysis of the other remaining channels becomes necessary to increase the sensitivity of different polarization and spin correlation observables to anomalous couplings. In the case of hadronic decay, final jet flavor tagging becomes essential to reconstruct the parity odd asymmetries. In our previous studies [24, 63], we have shown the effectiveness of machine learning techniques to tag the jets initiated by light quarks. A similar study of the semi-leptonic and hadronic decay of Z bosons will be reported elsewhere.

IV. CONCLUSION

In conclusion, we probe two processes viz. $e^-e^+ \rightarrow ZZ \rightarrow 4l$ and $e^-e^+ \rightarrow Z\gamma \rightarrow 2l\gamma$ for upcoming International Linear Collider (ILC) at center of mass en-

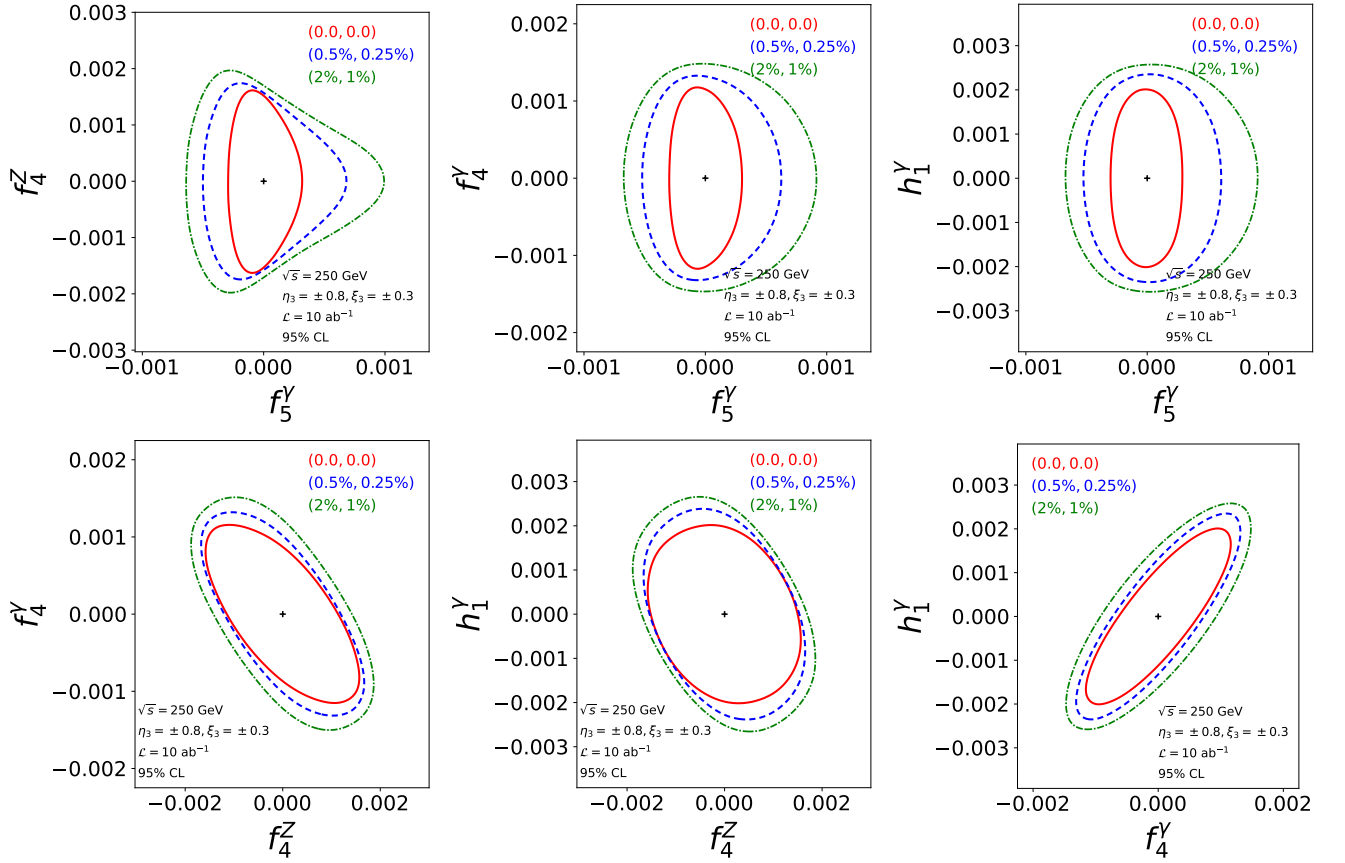


FIG. 8. Two dimensional projections of marginalized anomalous couplings at 95% CL for varying systematic error and integrated luminosity of 10 ab^{-1} .

ergy of 250 GeV with polarized beams in presence of four dimension-8 operators given in Eq. (4). These operators generates anomalous neutral triple gauge couplings ($Z^*ZZ, \gamma^*ZZ, \gamma^*Z\gamma$). To constrain the relevant Wilson coefficient, we construct polarization asymmetries of Z boson in case of $Z\gamma$ and for ZZ additional spin correlation asymmetries were also constructed. These observables were further divided into eight bins of $\cos\theta_Z$, where θ_Z is the angle between Z boson and the beam axis in the lab frame. In case of $Z\gamma$ process, there exist eight asymmetries in each bin where five are CP-even and three are CP-odd. While for ZZ process there are 80 asymmetries in each bin out of which 44 are CP-even and 36 are CP-odd. These CP-odd observables can be used to measure CP-violation in the production process. We used all these asymmetries along with cross section to put a simultaneous constrain on anomalous couplings using MCMC analysis. The final limits are obtained by combining $Z\gamma$ and ZZ process with two set of beam polarization at the level of χ^2 .

The limits on anomalous couplings c_i except for c_{BW} are dominated by the $Z\gamma$ process. The one parameter limits obtained in this work are tighter in the case of ZZ process, while for the $Z\gamma$ process, the limits are comparable to the LHC limits listed in Table I. The anomalous cou-

plings contain momentum-dependent terms normalized by the electroweak scale, making them more prominent at higher energy. Analysis at LHC also enjoys higher cross section for both ZZ and $Z\gamma$ process; thus, variable like cross section alone provides significant sensitivity to anomalous couplings. Thus, using many observables like polarizations and spin correlations becomes necessary to compensate for the low energy and cross section at ILC. Those observables could probe the CP structure of new physics. The current analysis could be extended by inculcating semi-leptonic and hadronic decay channels of Z bosons.

ACKNOWLEDGMENTS

A. Subba acknowledge University Grant Commission, Govt. of India, New Delhi for financial support through UGC-NET Senior Research Fellowship.

Appendix A: Anomalous couplings f_i^V, h_i^V

We use Eq. (7-10) to obtain the marginalized limits on f_i^V , and h_i^V by MCMC global fits. We list the marginal-

ized limits on four independent anomalous couplings in Table IV for different values of luminosity and systematic errors. In order to understand the behaviour of the anomalous couplings in presence of varying systematic errors, we show the marginalized two dimensional projection of four independent anomalous couplings at 95% CL in Fig. 8. The figures are obtained for different set of systematic errors and integrated luminosity of 10 fb^{-1} . The confidence interval for f_5^γ improved by a factor of ≈ 2.68 on decreasing the systematic from (2.0%, 1.0%) to zero. While for the CP -odd couplings, the confidence interval on f_4^Z gets tighter by a factor of ≈ 1.7 and simi-

larly for f_4^γ , and g_1^γ becomes better by a factor of ≈ 1.3 . The number suggest that the at the value of luminosity of 10 fb^{-1} , the limits become blind to the systematic errors except in case of one CP -even coupling. Similarly, if the luminosity increases by a factor of 100 while keeping the conservative value of systematic error, the limits on all the anomalous couplings gets better by a factor of approximately 3. The limits on these couplings can be probed to better precision with higher center of mass energy and increasing the polarization degree of positron which is one of the technological challenge for future electron-positron Collider.

-
- [1] G. Aad *et al.* (ATLAS), Observation of a new particle in the search for the Standard Model Higgs boson with the ATLAS detector at the LHC, *Phys. Lett. B* **716**, 1 (2012), [arXiv:1207.7214 \[hep-ex\]](#).
- [2] S. Chatrchyan *et al.* (CMS), Observation of a New Boson at a Mass of 125 GeV with the CMS Experiment at the LHC, *Phys. Lett. B* **716**, 30 (2012), [arXiv:1207.7235 \[hep-ex\]](#).
- [3] P. A. R. Ade *et al.* (Planck), Planck 2013 results. XVI. Cosmological parameters, *Astron. Astrophys.* **571**, A16 (2014), [arXiv:1303.5076 \[astro-ph.CO\]](#).
- [4] T. Aaltonen *et al.* (CDF), High-precision measurement of the W boson mass with the CDF II detector, *Science* **376**, 170 (2022).
- [5] B. Abi *et al.* (Muon g-2), Measurement of the Positive Muon Anomalous Magnetic Moment to 0.46 ppm, *Phys. Rev. Lett.* **126**, 141801 (2021), [arXiv:2104.03281 \[hep-ex\]](#).
- [6] H. Georgi, Effective field theory, *Ann. Rev. Nucl. Part. Sci.* **43**, 209 (1993).
- [7] S. Weinberg, Phenomenological Lagrangians, *Physica A* **96**, 327 (1979).
- [8] S. Weinberg, Effective Gauge Theories, *Phys. Lett. B* **91**, 51 (1980).
- [9] C. Degrande, A basis of dimension-eight operators for anomalous neutral triple gauge boson interactions, *JHEP* **02**, 101, [arXiv:1308.6323 \[hep-ph\]](#).
- [10] K. Hagiwara, R. D. Peccei, D. Zeppenfeld, and K. Hikasa, Probing the Weak Boson Sector in $e^+e^- \rightarrow W^+W^-$, *Nucl. Phys. B* **282**, 253 (1987).
- [11] G. J. Gounaris, J. Layssac, and F. M. Renard, Signatures of the anomalous Z_γ and ZZ production at the lepton and hadron colliders, *Phys. Rev. D* **61**, 073013 (2000), [arXiv:hep-ph/9910395](#).
- [12] M. Acciarri *et al.* (L3), Study of Z Boson Pair Production in e^+e^- collisions at LEP at $S^{(1/2)} = 189\text{-GeV}$, *Phys. Lett. B* **465**, 363 (1999), [arXiv:hep-ex/9909043](#).
- [13] G. Abbiendi *et al.* (OPAL), Study of Z pair production and anomalous couplings in e^+e^- collisions at $s^{*(1/2)}$ between 190-GeV and 209-GeV, *Eur. Phys. J. C* **32**, 303 (2003), [arXiv:hep-ex/0310013](#).
- [14] J. Alcaraz *et al.* (ALEPH, DELPHI, L3, OPAL, LEP Electroweak Working Group), A Combination of preliminary electroweak measurements and constraints on the standard model, (2006), [arXiv:hep-ex/0612034](#).
- [15] S. Chatrchyan *et al.* (CMS), Measurement of the ZZ Production Cross Section and Search for Anomalous Couplings in 2 l2l ' Final States in pp Collisions at $\sqrt{s} = 7 \text{ TeV}$, *JHEP* **01**, 063, [arXiv:1211.4890 \[hep-ex\]](#).
- [16] G. Aad *et al.* (ATLAS), Measurement of $W\gamma$ and $Z\gamma$ production cross sections in pp collisions at $\sqrt{s} = 7 \text{ TeV}$ and limits on anomalous triple gauge couplings with the ATLAS detector, *Phys. Lett. B* **717**, 49 (2012), [arXiv:1205.2531 \[hep-ex\]](#).
- [17] A. Collaboration, Evidence of pair production of longitudinally polarised vector bosons and study of cp properties in $zz \rightarrow 4\ell$ events with the atlas detector at $\sqrt{s} = 13 \text{ tev}$, (2023), [arXiv:2310.04350 \[hep-ex\]](#).
- [18] V. M. Abazov *et al.* (D0), Search for ZZ and $Z\gamma^*$ production in $p\bar{p}$ collisions at $\sqrt{s} = 1.96 \text{ TeV}$ and limits on anomalous ZZZ and $ZZ\gamma^*$ couplings, *Phys. Rev. Lett.* **100**, 131801 (2008), [arXiv:0712.0599 \[hep-ex\]](#).
- [19] T. Aaltonen *et al.* (CDF), Measurement of ZZ production in leptonic final states at \sqrt{s} of 1.96 TeV at CDF, *Phys. Rev. Lett.* **108**, 101801 (2012), [arXiv:1112.2978 \[hep-ex\]](#).
- [20] C. Degrande, C. Duhr, B. Fuks, D. Grellscheid, O. Mattelaer, and T. Reiter, UFO - The Universal FeynRules Output, *Comput. Phys. Commun.* **183**, 1201 (2012), [arXiv:1108.2040 \[hep-ph\]](#).
- [21] A. Alloul, N. D. Christensen, C. Degrande, C. Duhr, and B. Fuks, FeynRules 2.0 - A complete toolbox for tree-level phenomenology, *Comput. Phys. Commun.* **185**, 2250 (2014), [arXiv:1310.1921 \[hep-ph\]](#).
- [22] J. Alwall, M. Herquet, F. Maltoni, O. Mattelaer, and T. Stelzer, MadGraph 5 : Going Beyond, *JHEP* **06**, 128, [arXiv:1106.0522 \[hep-ph\]](#).
- [23] J. Alwall, R. Frederix, S. Frixione, V. Hirschi, F. Maltoni, O. Mattelaer, H. S. Shao, T. Stelzer, P. Torrielli, and M. Zaro, The automated computation of tree-level and next-to-leading order differential cross sections, and their matching to parton shower simulations, *JHEP* **07**, 079, [arXiv:1405.0301 \[hep-ph\]](#).
- [24] A. Subba and R. K. Singh, Role of polarizations and spin-spin correlations of W 's in $e^+e^- \rightarrow W^-W^+$ at $s=250 \text{ GeV}$ to probe anomalous W^-W^+Z/γ couplings, *Phys. Rev. D* **107**, 073004 (2023), [arXiv:2212.12973 \[hep-ph\]](#).
- [25] R. Rahaman and R. K. Singh, On polarization parameters of spin-1 particles and anomalous couplings in $e^+e^- \rightarrow ZZ/Z\gamma$, *Eur. Phys. J. C* **76**, 539 (2016), [arXiv:1604.06677 \[hep-ph\]](#).

TABLE IV. The translated marginalized 95% CL of anomalous couplings f_i^V, h_i^V (10^{-3}) at $\sqrt{s} = 250$ GeV with beam polarization $(\eta_3, \xi_3) = (\pm 0.8, \pm 0.3)$ from MCMC global fits for different values of luminosities and systematic error.

\mathcal{L} (fb $^{-1}$)	$(\epsilon_\sigma, \epsilon_A)$	f_3^γ	f_4^Z	f_4^γ	h_1^γ
100	(0.0, 0.0)	[-1.43, +1.52]	[-5.82, +5.50]	[-3.68, +3.66]	[-6.34, +6.26]
	(0.5%, 0.25%)	[-1.45, +1.55]	[-5.60, +5.52]	[-3.68, +3.66]	[-6.35, +6.27]
	(2.0%, 1.0%)	[-1.57, +1.72]	[-5.69, +5.65]	[-3.71, +3.67]	[-6.43, +6.32]
300	(0.0, 0.0)	[-1.00, +1.05]	[-4.10, +4.06]	[-2.77, +2.77]	[-4.72, +4.71]
	(0.5%, 0.25%)	[-1.05, +1.12]	[-4.12, +4.10]	[-2.79, +2.79]	[-4.77, +4.75]
	(2.0%, 1.0%)	[-1.22, +1.38]	[-4.26, +4.24]	[-2.81, +2.81]	[-4.87, +4.84]
1000	(0.0, 0.0)	[-0.65, +0.66]	[-2.87, +2.86]	[-1.99, +2.01]	[-3.38, +3.38]
	(0.5%, 0.25%)	[-0.74, +0.80]	[-2.91, +2.90]	[-2.02, +2.03]	[-3.47, +3.46]
	(2.0%, 1.0%)	[-0.92, +1.12]	[-3.05, +3.04]	[-2.07, +2.08]	[-3.60, +3.60]
3000	(0.0, 0.0)	[-0.42, +0.41]	[-2.02, +2.00]	[-1.44, +1.45]	[-2.44, +2.44]
	(0.5%, 0.25%)	[-0.56, +0.63]	[-2.07, +2.06]	[-1.50, +1.51]	[-2.61, +2.61]
	(2.0%, 1.0%)	[-0.74, +0.08]	[-2.18, +2.18]	[-1.58, +1.59]	[-2.76, +2.76]
10000	(0.0, 0.0)	[-0.25, +0.24]	[-1.29, +1.27]	[-0.94, +0.95]	[-1.64, +1.65]
	(0.5%, 0.25%)	[-0.44, +0.50]	[-1.35, +1.35]	[-1.08, +1.08]	[-1.94, +1.94]
	(2.0%, 1.0%)	[-0.57, +0.74]	[-1.51, +1.50]	[-1.22, +1.23]	[-2.14, +2.14]

- [26] R. Rahaman and R. K. Singh, On the choice of beam polarization in $e^+e^- \rightarrow ZZ/Z\gamma$ and anomalous triple gauge-boson couplings, *Eur. Phys. J. C* **77**, 521 (2017), [arXiv:1703.06437 \[hep-ph\]](#).
- [27] The International Linear Collider Technical Design Report - Volume 2: Physics, (2013), [arXiv:1306.6352 \[hep-ph\]](#).
- [28] The International Linear Collider Technical Design Report - Volume 3.II: Accelerator Baseline Design, (2013), [arXiv:1306.6328 \[physics.acc-ph\]](#).
- [29] T. K. Charles *et al.* (CLICdp, CLIC), The Compact Linear Collider (CLIC) - 2018 Summary Report **2/2018**, [10.23731/CYRM-2018-002](#) (2018), [arXiv:1812.06018 \[physics.acc-ph\]](#).
- [30] A. Abada *et al.* (FCC), FCC-ee: The Lepton Collider: Future Circular Collider Conceptual Design Report Volume 2, *Eur. Phys. J. ST* **228**, 261 (2019).
- [31] M. Demirci and A. B. Balantekin, Beam polarization effects on Z-boson pair production at electron-positron colliders: A full one-loop analysis, *Phys. Rev. D* **106**, 073003 (2022), [arXiv:2209.13720 \[hep-ph\]](#).
- [32] M. L. Swartz, PHYSICS WITH POLARIZED ELECTRON BEAMS, *Conf. Proc. C* **8708101**, 83 (1987).
- [33] S. H. Chen *et al.*, A toy Monte Carlo simulation for the transverse polarization of high-energy electron beams, *JINST* **17** (08), P08005.
- [34] K.-i. Hikasa, Effects of Transverse Polarization in Electron - Positron Collisions, *Phys. Lett. B* **143**, 266 (1984).
- [35] K.-i. Hikasa, Transverse Polarization Effects in e^+e^- Collisions: The Role of Chiral Symmetry, *Phys. Rev. D* **33**, 3203 (1986).
- [36] F. M. Renard, Single Transverse Polarization Effects in e^+e^- Collisions and the Structure of Chirality Violation, *Z. Phys. C* **45**, 75 (1989).
- [37] X.-K. Wen, B. Yan, Z. Yu, and C. P. Yuan, Single Transverse Spin Asymmetry as a New Probe of Standard-Model-Effective-Field-Theory Dipole Operators, *Phys. Rev. Lett.* **131**, 241801 (2023), [arXiv:2307.05236 \[hep-ph\]](#).
- [38] M. Placidi and R. Rossmanith, TRANSVERSE AND LONGITUDINAL POLARIZATION IN LEP, in *Conference on Tests of Electroweak Theories: Polarized Processes and Other Phenomena* (1985).
- [39] R. Barate *et al.* (ALEPH), Measurement of the $e^+e^- \rightarrow ZZ$ production cross-section at center-of-mass energies of 183-GeV and 189-GeV, *Phys. Lett. B* **469**, 287 (1999), [arXiv:hep-ex/9911003](#).
- [40] S. Schael *et al.* (ALEPH, DELPHI, L3, OPAL, LEP Electroweak), Electroweak Measurements in Electron-Positron Collisions at W-Boson-Pair Energies at LEP, *Phys. Rept.* **532**, 119 (2013), [arXiv:1302.3415 \[hep-ex\]](#).
- [41] J. Abdallah *et al.* (DELPHI), ZZ production in e^+e^- interactions at $s^{*}(1/2) = 183$ -GeV to 209-GeV, *Eur. Phys. J. C* **30**, 447 (2003), [arXiv:hep-ex/0307050](#).
- [42] T. A. Aaltonen *et al.* (CDF), Measurement of the ZZ production cross section using the full CDF II data set, *Phys. Rev. D* **89**, 112001 (2014), [arXiv:1403.2300 \[hep-ex\]](#).
- [43] V. M. Abazov *et al.* (D0), Measurement of the ZZ production cross section and search for the standard model Higgs boson in the four lepton final state in $p\bar{p}$ collisions, *Phys. Rev. D* **88**, 032008 (2013), [arXiv:1304.5422 \[hep-ex\]](#).
- [44] M. Aaboud *et al.* (ATLAS), $ZZ \rightarrow \ell^+\ell^-\ell'^+\ell'^-$ cross-section measurements and search for anomalous triple gauge couplings in 13 TeV pp collisions with the ATLAS detector, *Phys. Rev. D* **97**, 032005 (2018), [arXiv:1709.07703 \[hep-ex\]](#).

- [45] M. Aaboud *et al.* (ATLAS), Measurement of the $Z\gamma \rightarrow \nu\bar{\nu}\gamma$ production cross section in pp collisions at $\sqrt{s} = 13$ TeV with the ATLAS detector and limits on anomalous triple gauge-boson couplings, *JHEP* **12**, 010, [arXiv:1810.04995 \[hep-ex\]](#).
- [46] A. M. Sirunyan *et al.* (CMS), Measurements of the $pp \rightarrow ZZ$ production cross section and the $Z \rightarrow 4\ell$ branching fraction, and constraints on anomalous triple gauge couplings at $\sqrt{s} = 13$ TeV, *Eur. Phys. J. C* **78**, 165 (2018), [Erratum: *Eur.Phys.J.C* 78, 515 (2018)], [arXiv:1709.08601 \[hep-ex\]](#).
- [47] A. Yilmaz, A. Senol, H. Denizli, I. Turk Cakir, and O. Cakir, Sensitivity on Anomalous Neutral Triple Gauge Couplings via ZZ Production at FCC-hh, *Eur. Phys. J. C* **80**, 173 (2020), [arXiv:1906.03911 \[hep-ph\]](#).
- [48] A. Senol, H. Denizli, A. Yilmaz, I. Turk Cakir, K. Y. Oyulmaz, O. Karadeniz, and O. Cakir, Probing the Effects of Dimension-eight Operators Describing Anomalous Neutral Triple Gauge Boson Interactions at FCC-hh, *Nucl. Phys. B* **935**, 365 (2018), [arXiv:1805.03475 \[hep-ph\]](#).
- [49] S. Spor, Probe of the anomalous neutral triple gauge couplings in photon-induced collision at future muon colliders, *Nucl. Phys. B* **991**, 116198 (2023), [arXiv:2207.11585 \[hep-ph\]](#).
- [50] S. Jahedi and J. Lahiri, Probing anomalous $ZZ\gamma$ and $Z\gamma\gamma$ couplings at the e^+e^- colliders using optimal observable technique, *JHEP* **04**, 085, [arXiv:2212.05121 \[hep-ph\]](#).
- [51] S. Atag and I. Sahin, ZZ gamma and Z gamma gamma couplings at linear e^+e^- collider energies with the effects of Z polarization and initial state radiation, *Phys. Rev. D* **70**, 053014 (2004), [arXiv:hep-ph/0408163](#).
- [52] I. Ots, H. Uibo, H. Liivat, R. Saar, and R. K. Loide, Possible anomalous $Z Z$ gamma and Z gamma gamma couplings and Z boson spin orientation in $e^+e^- \rightarrow Z$ gamma, *Nucl. Phys. B* **702**, 346 (2004).
- [53] A. Gutierrez-Rodriguez, M. A. Hernandez-Ruiz, and M. A. Perez, Probing the ZZ gamma and Z gamma gamma Couplings Through the Process $e^+e^- \rightarrow \nu$ anti- ν gamma, *Phys. Rev. D* **80**, 017301 (2009), [arXiv:0808.0945 \[hep-ph\]](#).
- [54] J. Ellis, S.-F. Ge, H.-J. He, and R.-Q. Xiao, Probing the scale of new physics in the $ZZ\gamma$ coupling at e^+e^- colliders, *Chin. Phys. C* **44**, 063106 (2020), [arXiv:1902.06631 \[hep-ph\]](#).
- [55] A. Senol, H. Denizli, A. Yilmaz, I. Turk Cakir, and O. Cakir, The projections on $ZZ\gamma$ and $Z\gamma\gamma$ couplings via $\nu\bar{\nu}\gamma$ production in HL-LHC and HE-LHC, *Phys. Lett. B* **802**, 135255 (2020), [arXiv:1910.03843 \[hep-ph\]](#).
- [56] J. Ellis, H.-J. He, and R.-Q. Xiao, Probing neutral triple gauge couplings at the LHC and future hadron colliders, *Phys. Rev. D* **107**, 035005 (2023), [arXiv:2206.11676 \[hep-ph\]](#).
- [57] A. I. Hernández-Juárez, A. Moyotl, and G. Tavares-Velasco, Contributions to ZZV^* ($V = \gamma, Z, Z'$) couplings from CP violating flavor changing couplings, *Eur. Phys. J. C* **81**, 304 (2021), [arXiv:2102.02197 \[hep-ph\]](#).
- [58] A. I. Hernández-Juárez and G. Tavares-Velasco, Non-diagonal contributions to $Z\gamma V^*$ vertex and bounds on $Z\bar{l}q$ couplings, (2022), [arXiv:2203.16819 \[hep-ph\]](#).
- [59] R. Rahaman and R. K. Singh, Anomalous triple gauge boson couplings in ZZ production at the LHC and the role of Z boson polarizations, *Nucl. Phys. B* **948**, 114754 (2019), [arXiv:1810.11657 \[hep-ph\]](#).
- [60] F. Boudjema and R. K. Singh, A Model independent spin analysis of fundamental particles using azimuthal asymmetries, *JHEP* **07**, 028, [arXiv:0903.4705 \[hep-ph\]](#).
- [61] R. Rahaman and R. K. Singh, Breaking down the entire spectrum of spin correlations of a pair of particles involving fermions and gauge bosons, *Nucl. Phys. B* **984**, 115984 (2022), [arXiv:2109.09345 \[hep-ph\]](#).
- [62] R. Rahaman and R. K. Singh, Probing the anomalous triple gauge boson couplings in $e^+e^- \rightarrow W^+W^-$ using W polarizations with polarized beams, *Phys. Rev. D* **101**, 075044 (2020), [arXiv:1909.05496 \[hep-ph\]](#).
- [63] A. Subba and R. K. Singh, Study of anomalous $W^-W^+\gamma/Z$ couplings using polarizations and spin correlations in $e^-e^+ \rightarrow W^-W^+$ with polarized beams, (2023), [arXiv:2305.15106 \[hep-ph\]](#).